

Spitzer Mid-Infrared Spectroscopy of Infrared Luminous Galaxies at $z \sim 2$

L. Yan

*Spitzer Science Center, California Institute of Technology, MS 220-6,
Pasadena, CA 91125*

Abstract. We present the mid-IR spectra taken with the *Spitzer* InfraRed Spectrograph (IRS) for a sample of 52 infrared luminous, high redshift galaxies selected in the Extragalactic First Look Survey (XFLS). The target sample is selected to have $24\mu\text{m}$ flux densities brighter than 0.9mJy , and very red $24\mu\text{m}$ -to- $8\mu\text{m}$ and 24 -to- $8\mu\text{m}$ colors. The color criteria were designed to pick out high redshift sources with either PAH emission and/or steep mid-IR continua. Based only on the mid-IR PAH emission and silicate absorption features, we are able to derive redshifts for 48 ($48/52 = 92\%$) of the sources. The majority of these redshifts ($36/48 = 75\%$) are beyond $z = 1$, in the range of $1.2 \lesssim z \lesssim 3.2$. The Keck optical and near-IR spectroscopy of a subset has confirmed the mid-IR redshift identifications. The 52 spectra generally fall into three broad groups: (1) strong PAH emission, (2) heavily absorbed systems, and (3) mid-IR continuum dominated with weak PAH and/or silicate absorption features. Of the full sample, 35% have spectra with strong PAH emission (18/52, with 11 at $z \gtrsim 1.6$), 31% (16/52, at $1.77 \lesssim z \lesssim 3.2$) are heavily absorbed systems with strong silicate absorption at $9.8\mu\text{m}$ and also broad emission peak around $7.7\mu\text{m}$ (likely distorted PAH emission). The remainder 34% of the sample are mid-IR continuum dominated systems, where 14 spectra have weak PAH emission and/or silicate absorption (thus yielding redshifts), and 4 sources are without any identifiable features. The detections of deep silicate absorption galaxies imply that our sample has a significant population (at least 31%) of extremely luminous and heavily absorbed systems at $z \sim 2$. Combining the spectra and broad band photometries at $8\mu\text{m}$ and $70\mu\text{m}$, we fit the spectral continua and derived monochromatic, rest-frame $12\mu\text{m}$, continuum luminosities (νL_ν), ranging from $10^{11} - 10^{12.5} L_\odot$. The monochromatic $\nu L_\nu(12\mu\text{m})$ is crudely 1/10th of L_{ir} . Although our sample has a limited dynamic range in luminosity, we detect a weak trend that at the same redshift, sources with strong PAH emission tend to have lower luminosities than those of deeply embedded as well as continuum dominated systems.

1. Introduction

The peak of the far-infrared background detected by *COBE* is at $\sim 200\mu\text{m}$, with energy comparable to the optical/UV background Puget et al. (1996); Fixsen et al. (1998). This implies that $\sim 50\%$ of the integrated rest-frame optical/UV emission in the universe has to be thermally reprocessed by dust and radiated at the mid to far-infrared. Using the stacking technique, Dole et al. (2006) has recently quantified that $24\mu\text{m}$ sources with $S_{24\mu\text{m}} \sim 0.1 - 0.5\text{mJy}$ dominate the CIB emission at 70 & $160\mu\text{m}$. Deep ISO $15\mu\text{m}$ number counts, and more recently, *Spitzer* $24\mu\text{m}$ number counts, suggest a large excess of mid-IR sources compared

to the predictions by nonevolving models Marleau et al. (2004); Papovich et al. (2004); Gruppioni et al. (2002). Particularly, the *Spitzer* $24\mu\text{m}$ number counts imply that a significant population of sources with flux densities on the order of $100\mu\text{Jy}$ are likely infrared luminous galaxies at $z \sim 1 - 3$, previously undetected in the ISO data. Furthermore, the strong evolution of infrared luminous galaxies at $z \lesssim 1$ was directly characterized by the infrared luminosity functions (LF) Elbaz et al. (1999); Serjeant et al. (2000); Franceschini et al. (2002); Le Flo'ch et al. (2005). The LF determined recently from *Spitzer* data has shown that the turn-over of the LF, which marks the dominant contributors to energy density, moves higher with redshift, with the knee of infrared LF at $L_{\text{ir}} \sim (3 - 5)10^{11}L_{\odot}$ at $z \sim 1$ and $(3 - 5)10^{12}L_{\odot}$ at $z \sim 2$. At $z \sim 1$, LIRGs contribute to $70 \pm 15\%$ of the total (UV+IR) luminosity density (Le Flo'ch et al. 2005), and at $z \sim 2$, the ULIRGs volume density, is roughly two to three orders of magnitude higher in comparison with the local density of IRAS ultraluminous galaxies at the similar luminosity limit Soifer et al. (1987).

Although ISO and sub-mm observations have revealed many tantalizing facets of the dusty universe at $z \sim 1 - 3$, the successful launch of *Spitzer*, has made it possible to discover and characterize large numbers of infrared luminous galaxies beyond $z \sim 0.5$, where the mid-IR spectroscopic properties are virtually unknown. Low resolution, mid-IR spectra of IR luminous galaxies are dominated by the emission and absorption features of dust grains. While the shape of the mid-IR continuum and its brightness relative to the far-infrared constrain the amounts of hot and cold dust, the strong PAH emission features at $6.2, 7.7, 8.6, 11.3,$ and $12.7\mu\text{m}$ and silicate absorption (centered at 9.7 and $18\mu\text{m}$) provide both an indication of the type of source heating the dust (since PAH's are easily destroyed by UV photons and x-rays from an AGN) and redshift estimates for sources that are completely obscured at shorter wavelengths Genzel & Cesarsky (2000); Draine (2003); Laurent et al. (2000); Tran et al. (2001); Rigopoulou et al. (1999). The local infrared luminous galaxies show a large diversity in their mid-IR spectra, see Figure 1 in Spoon et al. 2005. With the sensitivity and wavelength coverage of the InfraRed Spectrograph (Houck et al. 2004, IRS;) on *Spitzer*, it is now possible to obtain the mid-IR spectral diagnostics of dusty galaxies out to $z \sim 3$. The existing *Spitzer* programs studying mid-IR spectra of high- z IR galaxies primarily target sources with relatively bright $24\mu\text{m}$ fluxes, on the order of 1mJy , with sample selections based on either $24\mu\text{m}$ or different wavelengths, such as sub-mm/mm or ISO. The $24\mu\text{m}$ selected surveys include GTO programs Houck et al. (30 spectra, $S_{24} > 0.75\text{mJy}$, $z \sim 2$) (2005), Weedman et al. (18, $> 1\text{mJy}$, $z \sim 2$) (2006), GO programs Le Flo'ch (12, $> 1\text{mJy}$, $z \sim 0.5 - 1.5$), Dole et al. (16, $z < 0.5$), Lagache et al. (40, $> 1\text{mJy}$, $z \sim 0.1 - 0.5$), Yan et al. (52, $> 1\text{mJy}$, $z \sim 1.5 - 2.6$, GO1) (2005,2006), Yan et al. (152, $> 1\text{mJy}$, $z \sim 1$, GO2). The SCUBA selected samples include Lutz et al. (2005a; GO1), Blain et al. (in progress, GO2), Chary et al. (in progress, GO2), and the Perez Fournon et al. sample (53, ISO selected, $S_{15\mu\text{m}} > 1\text{mJy}$).

2. The Mid-IR Spectroscopy of IR Luminous Galaxies in the FLS

In this talk, I will review the result from the GO1 Yan et al. program, which focuses on the mid-IR spectroscopy of luminous IR galaxies at $z \gtrsim 1$. This

program targeted a sample of 52 galaxies in the *Spitzer* First Look Survey (FLS)¹ over an area of 3.7deg^2 . The targets are potential starburst candidates at $z \gtrsim 1 - 2$ based on their mid-IR colors. In order to obtain good quality IRS spectra in reasonably short integration times, we required all spectroscopic targets to be brighter than 0.9mJy at $24\mu\text{m}$. We applied additional color constraints in order to select potential starburst galaxies at $z > 1$. This is based on $24/8$ and $24/0.7$ micron colors, requiring $R(24, 8) \equiv \log_{10}(\nu f_{\nu}(24\mu\text{m})/\nu f_{\nu}(8\mu\text{m})) \geq 0.5$, and $R(24, 0.7) \equiv \log_{10}(\nu f_{\nu}(24\mu\text{m})/\nu f_{\nu}(0.7\mu\text{m})) \geq 1.0$. The $R(24, 0.7) \geq 1.0$ condition is a crude redshift selection, and the $R(24, 8) \geq 0.5$ cutoff selects sources with very steep, red continua (see Yan et al. (2004) for details).

Of the total of 52 sources, we were able to derive redshifts for 48 sources based on either PAH emission and/or silicate absorption features. The 52 spectra are classified into three groups, with group 1 (strong PAH) containing 18 sources (18/52, with 11 at $z \gtrsim 1.6$), group 2 (strong silicate absorption and weak PAH) 16 sources (16/52, at $1.77 \lesssim z \lesssim 3.2$), group 3 (weak features (emission and absorption) and power-law continuum) 18 objects. Figure 1a,b,c and d shows examples of the IRS spectra for each of these three groups. We marked the PAH emission at $6.2, 7.7, 8.6, 11.2$ and $12.7\mu\text{m}$, and the broad absorption trough, roughly centered at the rest-frame wavelength of $9.7\mu\text{m}$. The redshift distribution for the 48 sources is shown in Figure 2. We also plotted the z -distribution for each source type (black for all, red for $t = 1$, green for $t = 1.5, 2$ and blue for $t = 3$). Of the 48 redshifts, 13 are $0.6 < z < 1.3$ and the remaining 35 are beyond $z = 1.5$. The dip at $1.3 < z < 1.6$ in Figure 2 is due to the fact that at $z = 1.5$, $24\mu\text{m}$ filter samples the rest-frame $9.6\mu\text{m}$, thus any samples with $24\mu\text{m}$ flux cutoff will inherently bias against selecting sources with $9.7\mu\text{m}$ silicate absorption around redshifts of 1.5.

The IRS spectra show that a large fraction of our sample (75%) are HyLIRGs with $L_{ir} \sim 10^{13}L_{\odot}$ at $z \sim 1.5 - 2.6$. It revealed the first direct evidence that PAH features are already a significant component of a dusty galaxy spectrum as early as $z=2$. We also found some indication that the properties of IR galaxies at high- z are different from that of the $z \sim 0$ counterparts. Specifically, among the 52 targets, 1/3rd are starbursts at $z \sim 2$ with strong PAH emission, and 2/3rd are AGN dominated systems with strong silicate absorption and weak or no PAH emission. The detailed results from this program are presented in Yan et al. (2006a).

2.1. Mid-IR Luminosities

The infrared luminosities of our sources ($L_{ir}(8 - 1000\mu\text{m})$) are in the range of $10^{12} - 10^{13}L_{\odot}$, but any accurate estimate of the bolometric luminosity requires data at rest-frame wavelengths longward of $60\mu\text{m}$. For our sample, we use mid-IR, $12\mu\text{m}$ continuum luminosities (monochromatic) to indicate the brightness of our sources. The crude relation is $L_{8-1000\mu\text{m}} \sim 15.85 \times L_{12}$. Figure 3 plots the L_{12} versus redshift for the different spectral types. The red and blue color indicates the sources with and without any PAH emission respectively. The dashed lines are the computed L_{12} vs. z relation if assuming a mid-IR spectrum like local

¹For details of the FLS observation plan and the data release, see <http://ssc.spitzer.caltech.edu/fls>.

ULIRG NGC6240 scaled to match the observed $F_{24\mu m}$ of 0.9mJy and 4.5mJy, the lower and upper limits of our sample. The peak and the valley at $z \sim 1.5$ and $z \sim 2$ reflect the silicate absorption trough and the strong $7.7 \mu m$ PAH emission passing through the observed $24 \mu m$ filter at these redshifts. In this figure, we see the general increase in luminosity with redshift as expected for a flux-limited selection, and more interestingly, the computed $L_{12} - z$ tracks match with the observed data points pretty well. We also note a weak trend in source-type with luminosity at a given redshift, *i.e.* strong AGN systems (blue symbols) tend to be brighter than the sources with PAH emission (red symbols). Our sample is not ideal for studying this relation because of its limited dynamic range in luminosity, limited by the fact that most of our sources have $24 \mu m$ flux densities around 1mJy. The brightest to faintest galaxies differ by at most about a factor of 5, with only a handful approaching the brighter end. Nevertheless, Fig. 3 suggests a vague trend that at $z \sim 2$, PAH-dominated sources tend to be the least luminous, while continuum-dominated sources tend to be somewhat more luminous. Type 1.5, having both strong continuum and strong PAH tends to be intermediate. Studies of local ULIRGs suggest that above $\sim 10^{12.5} L_{\odot}$, ULIRGs tend to be AGN-dominated (Lutz et al. 1998). At $z \gtrsim 1$, *all* our galaxies are above this limit. Therefore if the above (marginal) trend is confirmed, then we are seeing the same trend of AGN-activity increasing with luminosity except the transition luminosity is higher. This luminosity evolution with redshift is also reflected by the fact that our $z \sim 2$, PAH-dominated systems seem to be more luminous by ~ 0.5 dex than local starburst ULIRGs. This immediately begs the question whether the physical mechanism, which generates this tremendous energy output is the same for $z = 2$ and $z = 0$ starburst ULIRGs. The answer to this important question will come in next few years when we have more comprehensive analyses of this sample using multi-wavelength data.

Because the GO1 sources are color-selected, our GO2 program was designed to obtain low resolution IRS spectra for 152 sources, a flux limited sample with $S_{24\mu m} \gtrsim 1$ mJy. The first set of observations (69 spectra) has been reduced. The redshift distribution shows that a large fraction of these sources are $z \sim 1$ ULIRGs (their $S_{24\mu m} \gtrsim 1$ mJy). Initial analysis shows that many of these $z \sim 1$ spectra have strong PAH, and some with only deep silicate absorption. The GO1 and GO2 spectra provide a large dataset, characterizing the mid-IR spectral properties for galaxies at $L_{ir} \sim 10^{12}$ and $10^{13} L_{\odot}$ at $z \sim 1$ and 2, respectively. The detailed results from this program are presented in Yan et al. (2006a).

3. Millimeter and Optical/near-IR Spectroscopic Follow-up Observations

We have started to obtain 1.2mm continuum observations of the GO1 IRS sample. The half of this sample has been observed with MAMBO on IRAM 30meter telescope. The detailed descriptions of the observation and analyses are in Lutz et al. (2005b). The 1.2mm sample is selected to target a subset of 40 bright ($S_{24\mu m} > 1$ mJy) sources that are optically faint, as evidenced by a $24\mu m$ to optical ‘color’ $R(24, 0.7) \equiv \log_{10}(\nu F_{\nu}(24\mu m)/\nu F_{\nu}(0.7\mu m))$ of at least 1 ($R > 22.5$ for $S_{24\mu m} = 1$ mJy). Each source has roughly about 1.5hours of on-target integration, with rms noise of 0.66mJy. The sample as a whole is well detected at

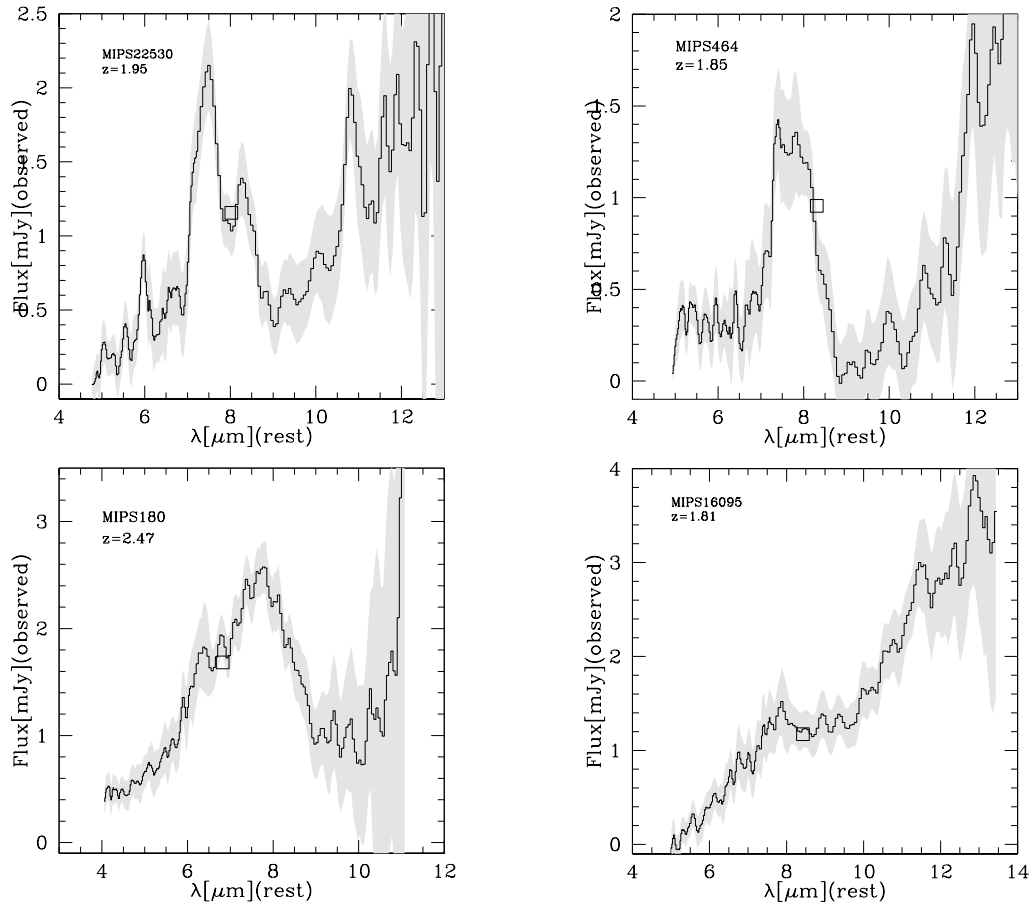


Figure 1. The four panels show example spectra.

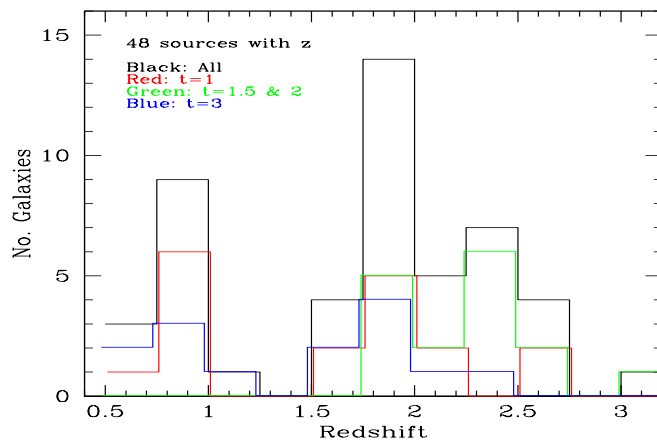


Figure 2. Redshift distribution of 48 out of the 52 GO1 sample. These redshifts are purely based on the mid-IR spectral signatures.

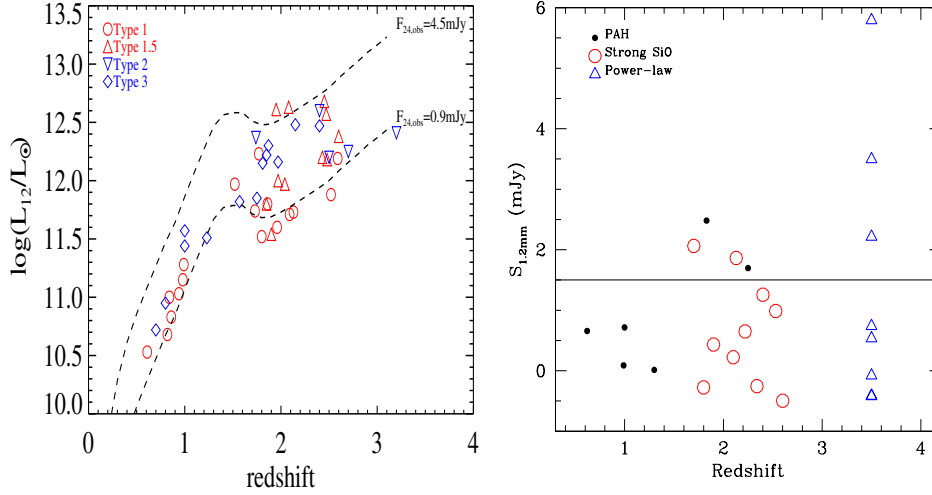


Figure 3. – **Left:** Monochromatic $12\mu\text{m}$ luminosity vs. redshift with different symbols marking the different source types. The red and blue color crudely separates the sources with starbursts and strong AGN respectively. The dashed line shows the L_{12} vs. z relation if we take a SED like NGC6240 with the $F_{\text{obs}}(24\mu\text{m})$ scaled to the lower and upper limits of our survey sample. Figure 4 – **Right:** The 1.2mm fluxes measured from MAMBO/IRAM versus redshifts determined from the IRS spectra. As shown, a small fraction of our sample are detected at 1.2mm continuum. This implies that at $L_{\text{ir}} \sim 10^{13}L_{\odot}$, a large fraction of $24\mu\text{m}$ selected populations have dust obscured, strong AGN components.

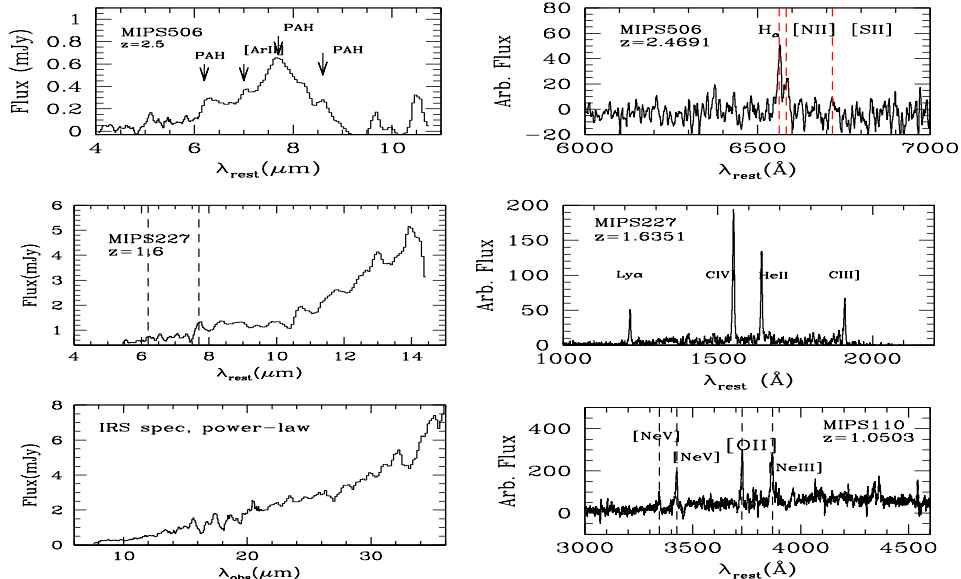


Figure 5. Three examples of keck spectra, one for each instrument — NIR-SPEC, LRIS and DEIMOS. We plot the mid-IR data together with the Keck spectrum for each source.

mean $S_{1.2mm} = 0.74 \pm 0.09$ mJy and $S_{1.2mm}/S_{24\mu m} = 0.15 \pm 0.03$. Seven (three) of the sources are individually detected at $> 3\sigma$ ($> 5\sigma$) levels. Mean millimeter fluxes are higher for sources with the reddest mid-infrared/optical colors. Figure 4 shows the 1.2mm fluxes versus the redshifts determined for some of the GO1 sample which we have 1.2mm measurements. We found that at the 3σ limit of 1.98mJy, majority of our GO1 sources are not detected at 1.2mm. This probably implies that sources with $24\mu m$ flux density of 1mJy or brighter could have substantial AGN populations. Although more detailed SED analyses, including the proper redshift information are necessary in order to conclude the AGN contribution to bolometric luminosities for individual sources. The complete observations of the GO1 sample will be done in 2006, and we should have better statistics of the fraction of sources with mm emission.

We obtained optical and near-IR spectra for 28 sources from our IRS sample using the instruments (LRIS, DEIMOS and NIRSPEC) on the Keck telescopes. From these data, we were able to determine redshifts for 18 of these sources. All of the Keck redshifts confirm the estimates based only on the mid-IR features. The rest-frame UV/optical emission lines detected in the Keck spectra are mostly also consistent with the source classification suggested by the mid-IR spectra. The detailed analyses of this data will be in a separate paper (Yan et al. 2006b, in preparation). Figure 5 shows three examples of Keck spectra, one per each instrument (NIRSPEC, LRIS and DEIMOS). Of the 8 sources observed by NIRSPEC, we were able to detect $H\alpha$ emission line for 6 of them with $1.8 < z < 2.6$. The rest-frame FWHM of $H\alpha$ line in all 6 sources are fairly narrow, less than 1000 km/second. The $[NII]/H\alpha$ ratios are in the range of 0.1–0.3, which span the range of values for both starbursts and Seyfert II. Additional near-IR spectroscopy, covering both $H\alpha$ and $[OIII]5007$, have been scheduled for more sources from our IRS sample. Using LRIS and DEIMOS, we were able to measure redshifts for 6 and 5 sources respectively, mostly at $z \sim 1$. The additional spectroscopy of the whole IRS sample has been planned in 2006.

4. Cosmological Implications

The detections of infrared luminous galaxies at $z \sim 2$ based on only mid-IR spectra have several significant implications for studies of galaxy evolution at high redshifts. As a benchmark for comparison, the comoving number density of sub-mm detected galaxies at $\langle z \rangle = 2.2$ and $1 < z < 3$ is roughly $6 \times 10^{-6} \text{Mpc}^{-3}$ for $L_{ir} \geq 4 \times 10^{12} L_{\odot}$ (Chapman et al. 2004), and the the rest-frame UV color selected galaxies have co-moving space density of $2 \times 10^{-3} \text{Mpc}^{-3}$ for both the BM ($\langle z \rangle = 1.77$) and BX ($\langle z \rangle = 2.32$) selection (Aldelberger et al. 2004). It is worth pointing out that although optically faint, radio selected SCUBA galaxies tend to have the rest-frame UV colors satisfying the BX and BM criteria, they have much fainter R -band magnitude (Chapman et al. 2003). Although our current sample is very small, it would be illustrative to compute the comoving number density of infrared luminous galaxies at $z \sim 2$. Our crude estimation is as follows. Among all of the $24\mu m$ sources over the area we studied (3.7 deg^2), 59 sources satisfies our sample selection conditions. If we assume 75% of these 59 sources being at $z = 2.0 \pm 0.3$, the comoving number density is $n = N/V_c \sim 2 \times 10^{-6} \text{Mpc}^{-3}$ for $z = 2$ and $L_{IR} \geq 5 \times 10^{12} L_{\odot}$. Given the large

uncertainties, our estimate is probably consistent with that of sub-mm sources and is roughly 1% of the UV selected $z \sim 2$ galaxies. The exact relation between our sample and SCUBA sources would require future work to quantify. We note that the bolometric infrared luminosity of UV selected galaxies at $z \sim 2 - 3$ is roughly $10^9 - 10^{10} L_{\odot}$ (Adelberger & Steidel 2000), 3-4 orders of magnitude less than those of our sources. Therefore, galaxies like ones from our sample could contribute significantly to the total luminosity density at high redshift.

Acknowledgments. We are grateful to the IRS instrument team and the IRS instrument support team at the Spitzer Science Center for their tremendous effort to make this instrument such a great success. We also thank H. Teplitz for organizing this successful conference, where we saw many exciting new *Spitzer* results.

References

- Adelberger, K. L., et al. 2004, ApJ, 607, 226
 Adelberger, K. L., & Steidel, C. C. 2000, ApJ, 544, 218
 Armus, L. et al. 2004, ApJS, 154, 178
 Chapman, S. C., Smail, I., Blain, A. W., & Ivison, R. J. 2004, ApJ, 614, 671
 Chapman, S.;Blain,A.W.;Ivison,R.J.;Smail,I.R. 2003, Nature, 422, 695
 Dole, H. et al. 2006, \dot{a} , in press
 Draine, B. T. 2003, ARA&A, 41, 241
 Elbaz et al. 1999, A&A, 351, 37
 Fixsen,D.J.; Dwek,E.; Mather,J.C.;Bennett,C.J.;Shafer,R.A. 1998, ApJ, 508, 123
 Franceschini et al. 2002, ApJ, 568, 470
 Genzel, R. & Cesarsky, C.J. 2000, ARA&A, 38, 761
 Gruppioni et al. 2002, MNRAS, 335, 831
 Houck, J. R., et al. 2004, ApJS, 154, 18
 Houck, J. R., et al. 2005, ApJL, 622, 105
 Laurent, O. et al. 2000, A&A, 359, 887
 Le Flo'ch, E. et al. 2005, ApJ, 632, 169
 Lutz, D., Yan, L. et al. 2005, ApJ, 632, 13
 Lutz, D. et al. 2005, ApJ, 625, 83
 Lutz, D., Spoon, H. W. W., Rigopoulou, D., Moorwood, A. F. M., & Genzel, R. 1998, ApJ, 505, L103
 Marleau, F. R., et al. 2004, ApJS, 154, 66
 Papovich, C., et al. 2004, ApJS, 154, 70
 Puget,J.-L.;Abergel, A.; Bernard,J.-P. et al. 1996, A&A, 308L, 5
 Serjeant et al. 2000, MNRAS, 317, 29
 Soifer, B. T., Sanders, D. B., Madore, B. F., Neugebauer, G., Danielson, G. E., Elias, J. H., Lonsdale, C. J., & Rice, W. L. 1987, ApJ, 320, 238
 Spoon, H.W.W. et al. 2004, ApJS, 154, 184
 Spoon, H. W. W. et al. 2005, astro-ph/0512037.
 Tran, Q. D., et al. 2001, ApJ, 552, 527
 Weedman, D. et al. 2006, ApJ, 638, 613
 Werner, M. W., et al. 2004, ApJS, 154, 1
 Yan, Lin et al. 2004, ApJS, 154, 60
 Yan, Lin et al. 2005, ApJ, 624, 608
 Yan, Lin et al. 2006a, ApJ, submitted
 Yan, Lin et al. 2006b, ApJ, in preparation.